Springer

Journal of
Mechanical
Science and
Technology

Journal of Mechanical Science and Technology 22 (2008) 798~811

www.springerlink.com/content/1738-494x

Amplification effect of redistribution from elliptic relaxation equation with Reynolds stress model in rotating flow

Kun-Ho Chun[1], Young-Don Choi[2,*], Jong-Keun Shin[3] and Tae-Hyun Chun[1]

[1]*Korea Atomic Energy Research Institute, P.O. Box 105, Yusong, Daejon, Korea, 305-600*
[2]*Department of Mechanical Engineering, Korea University, 1, 5-Ka, Anam-dong Sungbuk-ku, Seoul, 136-701, Korea*
[3]*Department of Automotive Engineering, Donghae University, 119 Jiheungdong, Donghae Kangwondo, 240-713, Korea*

(Manuscript Received July 4, 2007; Revised December 27, 2007; Accepted December 27, 2007)

Abstract

A new elliptic relaxation operator that is able to correct the erroneous increase of the redistribution from the original one suggested by Durbin [J. Fluid Mech. 249], is developed by using an inhomogeneous correction to its source term. In this work the amplification of the redistribution arising from the original model is investigated in detail by using DNS analysis. It is shown that the amplification effect extends the near-wall layer into the wake layer as well as the logarithmic layer. Also, it can be seen that the remedy of all modified neutral operators proposed so far is limited only in the logarithmic layer. However, the behavior of the present operator can be significantly improved in the overall region without amplification of the redistribution. The computational results for the new operator agree quite well with the DNS/LES data without using any ad hoc additional term in the governing equations in order to obtain a rotating effect.

Keywords: Elliptic relaxation equation; Reynolds stress model; Rotating flow; Redistribution; Length scale

1. Introduction

In computational fluid dynamics (CFD), turbulence models using the Reynolds-Averaged Navier-Stokes (RANS) equation are widely employed in order to predict complex engineering flows. Current engineering approximation for the RANS model is divided into an isotropy one and an anisotropy one. Although isotropy models, such as two-equation eddy-viscosity models (EVM) etc., are unable to capture many important physical phenomena including rotation, buoyancy and streamline curvature, etc., they have been employed as a major tool in engineering applications due to their numerical stability, low computational cost and simple implementation. On the other hand, anisotropy models such as the Reynolds stress equation model (RSM), algebraic stress model (ASM) etc. account for the effects of stress anisotropy and are regarded as the natural and most logical models to predict many physical effects. However, there still are several difficult issues like pressure dominated flows and the treatment of near wall flows, which often diminishes the inherent superiority of the RSM as compared with EVM, leading to an erroneous judgment.

In the Reynolds stress equation model, the near-wall turbulence modeling remains a challenging assignment for statistical modeling because the near-wall region is characterized by a strong inhomogeneity and anisotropy due to the sharp gradients of the mean shear and turbulence statistics. In particular, the modeling of the pressure gradient-velocity correlation is the primary task since the presence of a wall brings about a strong inhomogeneous and anisotropic turbulence. Most of the models for the pressure gradient-velocity correlation used so far are based on a quasi-homogeneous and local assumption [1, 2]. This term

*Corresponding author. Tel.: +82 2 3290 3355, Fax.: +82 2 928 1067
E-mail address: ydchoi@korea.ac.kr
DOI 10.1007/s12206-007-1214-3

is generally divided into slow, rapid and wall-reflection parts. The first two terms, which are called 'pressure-strain' correlation, are related to the volume integrals of the two-point correlation between velocities and the pressure gradient, whereas the third term, which is called 'wall echo' correlation, is the surface integral. Many previous works for modeling each term have proposed models for satisfying the geometric or kinematic constrains such as a realizability condition and Caley-Hamilton theorem. A number of them employed an arbitrary function in the slow part for satisfying the two-component turbulent limit in the near-wall region. But these models cannot generally be integrated down to solid boundaries, so they fail to predict the correct behaviors of the near-wall turbulence statistics. In order to correct the spurious behavior of the pressure-strain correlation in the near-wall region, quasi-homogeneous approximations have led to the use of an ad hoc wall echo model for selectively damping the velocity fluctuations in the wall-normal direction only. But these methods have difficulty in modeling the wall-echo term, which sometimes causes a numerical instability and difficulty in application. Therefore, modeling for the pressure gradient-velocity correlation still remains a challenging problem.

In order to avoid the use of these damping functions, Launder and Tselepidakis [3] and Launder & Li [4] proposed redistribution models that include an effective velocity gradient instead of the wall-echo term. A quasi-homogeneous model using the normalized length scale gradients for the pressure-strain correlation was also proposed by Craft & Launder [5], which can be integrated down to solid boundaries without having damping functions. These models are of a parabolic character that can be described by an algebraic expression. However, the pressure-strain correlation has an elliptic character that can't be simply determined by a linear expression [6].

In contrast to this local assumption, Durbin [6, 7] proposed a way to account for the non-local character and the near-wall inhomogeneity by solving an elliptic relaxation equation that is inverted by a modified Helmholtz equation. The former is preserved through the elliptic relaxation operator and the latter can be integrated down to the wall through the use of the boundary conditions without using the damping function. One outstanding feature of the elliptic relaxation approach is that it accounts for the wall blocking effect that restrains the velocity fluctuations normal to the wall and that reflects the pressure fluctuations by the wall. This wall blocking effect, which induces an energy transfer from the wall-normal component to the other ones, has an effect at significant distances from the wall through the pressure field, and it reproduces quite satisfactorily the inhomogeneous and anisotropic turbulence characteristics in the near-wall region [6-8].

However, Wizman et al. [9] showed that the original elliptic operator induces an amplification of the redistribution since this operator does not correctly behave in the logarithmic layer. Manceau et al. [8] also showed that the spurious behavior of the original elliptic operator is due to the symmetric correlation function used for deriving the elliptic relaxation equation, which does not account for the asymmetry of the two-point correlations involved in the integral equation of the redistribution term. In order to correct the drawback of the standard model, new elliptic operators were derived by some works [8-12]. For the behavior of these modified elliptic operators, they will be examined in detail by using the DNS analysis in order to understand their amplification from the elliptic relaxation equations. In particular, it is of interest to examine the fully developed spanwise rotating channel flow due to the substantially different turbulence quantities on both sides of the channel. That is, when the rotation rates are increased, the turbulence is gradually enhanced on the pressure side and reduced on the suction side. After all, the energy containing eddies become much smaller and eventually disappear due to a thickening of the relaminarized region on the suction side [13, 14].

The main objective of the present study is to explore a new neutral formulation that is able to eliminate the spurious behavior of the redistribution from the elliptic relaxation equation. The development of this operator is given in section 2. In order to evaluate this model, DNS analyses are conducted in section 3. The applications for the assessment of this operator are finally performed in a plane channel flow and spanwise rotating channel flow at higher and wider rotation numbers in section 4. The starting point of this work is to confirm the amplification of the redistribution arising from the existing elliptic relaxation operators by the DNS data [15, 16]. Also, the amplification effects for the length scale will be presented in section 3.

2. The modification of the elliptic relaxation equation

It is useful in the present section to briefly outline the method of deriving the elliptic relaxation equation proposed by Durbin [6, 7]. The pressure gradient-velocity correlation in the Reynolds stress transport equation is

$$\rho\Pi_{ij} = -\left(\overline{u_i \frac{\partial p}{\partial x_j}} + \overline{u_j \frac{\partial p}{\partial x_i}} \right), \tag{1}$$

which is modeled by the integral equation as

$$\rho\Pi_{ij} = -\int_{\Omega} \frac{\Psi_{ij}(\mathbf{x},\mathbf{x}')}{4\pi \left\| \mathbf{x}-\mathbf{x}' \right\|} dV(\mathbf{x}') \tag{2}$$

$\Psi_{ij}(\mathbf{x},\mathbf{x}')$ here is the two-point correlation between the fluctuating velocity and the Laplacian of the pressure gradient. Here Durbin assumes the two-point correlation as an exponential function:

$$\Psi_{ij}(\mathbf{x},\mathbf{x}') = \Psi_{ij}(\mathbf{x}',\mathbf{x}') \cdot f(\mathbf{x},\mathbf{x}') \tag{3}$$

where

$$f(\mathbf{x},\mathbf{x}') = \exp\left(\frac{-\left|\mathbf{x}'-\mathbf{x}\right|}{L} \right) \tag{4}$$

L is the correlation length scale. The integral of Eq. (2) involving the exponential function (4) is inverted by a modified Helmholtz equation ($\nabla^2 - 1/L^2$),

$$\Pi_{ij} - L^2\nabla^2\Pi_{ij} = -\frac{L^2}{\rho}\Psi_{ij}. \tag{5}$$

Where the source term Ψ_{ij} should be modeled. Durbin [6] assumes that in the homogeneous situation this term can be replaced by the homogeneous model Π_{ij}^h. For this source term the present work adopts an assumption of the inhomogeneous situation unlike the original model. Here we here assume that this term is achieved by being decomposed into the homogeneous and inhomogeneous parts as follows:

$$-\frac{L^2}{\rho}\Psi_{ij} = \underbrace{\left(\Pi_{ij}^h - L^2\nabla^2\Pi_{ij}^h\right)}_{homogenious\ \ part} + \underbrace{\left(\Pi_{ij}^{inh} - L^2\nabla^2\Pi_{ij}^{inh}\right)}_{inhomogenious\ \ part}. \tag{6}$$

Each first term in the parentheses on the right-hand sides in Eq. (6) can be replaced by any quasi-homogeneous pressure-strain model,

$$\Pi_{ij}^h + \Pi_{ij}^{inh} \cong \Pi_{ij}^{qh}. \tag{7}$$

In eq. (6) $L^2\nabla^2\Pi_{ij}^h$ vanishes in itself. $L^2\nabla^2\Pi_{ij}^{inh}$ is assumed by the following approximation,

$$\nabla^2\Pi_{ij}^{inh} = \left[(1-\sigma) \ \left(\nabla^2\Pi_{ij}^{inh}\right)_{inner\ \ region} + \sigma \ \left(\nabla^2\Pi_{ij}^{inh}\right)_{outer\ \ region} \right]. \tag{8}$$

The parameter σ may be used to adjust the pressure gradient-velocity correlation in the logarithmic layer where there is a common region between the inner and outer layers. In order to model the first term of the right-hand side, we introduce the following approximation:

$$\left[\nabla^2\Pi_{ij}^{inh}\right]_{inner\ \ region} = \frac{1}{L^2}\left[L^2\nabla^2\Pi_{ij} - \nabla\circ(L^2\nabla\Pi_{ij})\right]. \tag{9}$$

In the logarithmic layer, assuming that Π_{ij} behaves as $1/y$ and the length scale is $L = \kappa y$ (κ is Von-Karman's constant), the first term of the right-hand side is the original operator [7] and the second term is a neutral operator [11]. Here, we believe that the difference between two operators reflects correctly the inhomogeneous effects of the redistribution in the logarithmic layer. On the other hand, the second term of Eq. (8) can be reconstructed by adding the term $\nabla^2\Pi_{ij}^h$ which is assumed to have vanished.

$$\left[\nabla^2\Pi_{ij}^{inh}\right]_{outer\ \ region} = \left[\nabla^2\Pi_{ij}^{inh}\right]_{outer\ \ region} + \ \nabla^2\Pi_{ij}^h \cong \nabla^2\Pi_{ij}. \tag{10}$$

Thus, substituting Eqs. (7)~(10) into Eq. (6), the right-hand side of a modified Helmholz equation Eq. (5) yields the following form:

$$-\frac{L^2}{\rho}\Psi_{ij} = \Pi_{ij}^{qh} + (1-\sigma)\nabla\circ(L^2\nabla\Pi_{ij}) - L^2\nabla^2\Pi_{ij}, \tag{11}$$

where

$$L^2\nabla^2\Pi_{ij} = (1-\sigma) \ \left[L^2\nabla^2\Pi_{ij}\right] + \sigma\left[L^2\nabla^2\Pi_{ij}\right]. \tag{12}$$

Now, let us replace the right-hand side of Eq. (5) by Eq. (11), thus a new formulation of the elliptic relaxation operator can be derived as

$$\Pi_{ij} - (1-\sigma \ )\nabla\circ(L^2\nabla\Pi_{ij}) = \Pi_{ij}^{qh}. \tag{13}$$

This differential equation model of a pressure gradient-velocity correlation preserves the non-local characteristic and accounts for the reproduction of the wall blocking effect by applying its boundary condition that is not driven by Π_{ij}, but by the relaxation redistribution tensor $\wp_{ij}$.

$$\wp_{ij} = \Pi_{ij} - \varepsilon_{ij} + \frac{\overline{u_i u_j}}{k}\varepsilon. \tag{14}$$

In the near-wall region the behavior of the Reynolds stress transport equation is satisfied by $\Pi_{ij} - \underline{\varepsilon_{ij}} = -D_{ij}$ and $\Pi_{ij} = n\varepsilon_{ij}$ (for example, $n = -1/2$ for v^2). Substituting $\wp_{ij}$ by kf_{ij} for the resolution of the elliptic equation and ε_{ij} by $2/3\varepsilon\delta_{ij}$ in a homogeneous approach, the elliptic equation finally takes the following form:

$$f_{ij} - (1-\sigma)\nabla \circ (L^2 \nabla f_{ij}) = \frac{\Phi_{ij}^{qh}}{k} + \frac{2b_{ij}}{T}. \tag{15}$$

where

$$\sigma = 4b_{ij}b_{ji}, \text{ where } b_{ij} = \frac{\overline{u_i u_j}}{2k} - \frac{1}{3}\delta_{ij} \tag{16}$$

$$L = C_L \max\left(\frac{k^{3/2}}{\varepsilon},\ C_\eta \left(\frac{\nu^3}{\varepsilon} \right)^{1/4} \right), \tag{17}$$

$$T = \max\left(\frac{k}{\varepsilon},\ C_T \left(\frac{\nu}{\varepsilon} \right)^{1/2} \right). \tag{18}$$

Here L and T are the length and time scales in conjunction with the Kolmogorov scale in the near-wall region, respectively. Π_{ij}^{qh} is decomposed into a pressure-strain correlation Φ_{ij}^{qh} and a pressure diffusion D_{ij}^{p}. In the outer region of a channel flow the pressure diffusion is negligible unlike the boundary condition, so Π_{ij}^{qh} is replaced by Φ_{ij}^{qh}, which is also called a redistribution term due to the energy redistribution between Reynolds stress components. The parameter $(1-\sigma)$ has a role in eliminating and correcting the erroneous behavior of the redistribution in the outer layer due to the strong wall blocking effect of the elliptic relaxation equation model at the wall.

3. The behavior of the elliptic operators using DNS data

3.1 Amplification factor

The elliptic relaxation Eq. [7], which is developed as the alternative to a near-wall damping function or the "wall-echo term, evidently improves the behavior of the pressure-strain correlation in the region near the wall. However, the original model still remains to be modified in the logarithmic region due to an amplification of the redistribution, as mentioned by Manceau et al. [8] and Wizman et al. [9]. Their remedy for this behavior was a neutral type of the elliptic operator. Laurence & Durbin [11] were the first to propose a neutral elliptic operator (hereafter, LD), as arranged in Table 1. Thereafter, Durbin & Laurence [10] proposed another operator (DL) rescaled by $\wp_{ij} = kf_{ij}/L$ and the new length scale modeled by the sum of the Kolmogorov length scale and the turbulent length scale. Wizman et al. [9] showed that the original elliptic operator tends to increase slightly the slow term through standard wall echo corrections. They suggested a reformulated neutral elliptic relaxation operator by introducing the concept of a gradient of the length scale (W1, W2). In particular, Manceau et al. [8] proposed very theoretically a neutral operator in the logarithmic layer. They showed that the correlation function has the characteristic of asymmetry due to the strong inhomogeneity in the vicinity of the wall by the DNS channel flow database analysis and derived the new formulation (M2) by using the asymmetrical shape of the correlation function $L + \beta(\mathbf{x}' - \mathbf{x}) \cdot \nabla L$ instead of L in Eq. (4). They also proposed another new model (M1) to correct the inversion error, which is based on the observation that the length scale cannot be considered locally as a constant.

The definition of a neutral or non-neutral operator indicated in Table 1 is decided by whether the amplification factor Γ from $\Phi_{ij}^{*} = \Gamma\Phi_{ij}^{h}$ is "unity" in the logarithmic layer or not, as mentioned by Manceau et al. [8]. This analysis is based on the logarithmic layer assumptions: $\Phi_{ij}^{h} = C/y$, $k = u_\tau^2/C_\mu^{1/2}$ and $\varepsilon = u_\tau^3/\kappa y$. Here Φ_{ij}^{*} is not the exact solution of the differential

Table 1. The model coefficients and operator types of the elliptic relaxation equation.

Model	Elliptic Relaxation Equation			Length scale		Operator type
	α_1	α_2	α_3	C_L	C_η	Γ
Present	1	$8B_2$	$4B_2$	0.2	80	Neutral
D [7]	1	0	1	0.2	80	Non-neutral
LD [11]	1	2	1	0.2	80	Neutral
DL [10]	$1 - L\nabla^2 L$	2	1	0.2*	60*	Neutral
W1 [9]	$1 - 2(\nabla L)^2 - 2L\nabla^2 L$	4	1	0.29	80	Neutral
W2 [9]	$1 - 2L\nabla^2 L - 2L^2 \nabla L \circ \nabla(1/L)$	2	1	0.2	80	Non-neutral
M1 [8]	1	1	1	0.2	80	Non-neutral
M2 [8]	$1+16\beta(\nabla L)^2$	8β	1	0.28	80	Neutral

Note: * $L = C_L^2 \left(\frac{k^3}{\varepsilon^2} + C_\eta^2 \frac{\nu^{3/2}}{\varepsilon^{1/2}} \right)$

equation, but only a particular solution without considering its boundary condition. Note that this amplification factor does not account for the behavior of the redistribution in the near-wall and wake region and also is not affected by the length scale. The aim in using this factor is to classify the elliptic relaxation operators. As a result, in order to examine the entire region of the flow field, it is necessary to introduce a new amplification tensor factor.

In order to investigate the amplification effects of these elliptic operators, we will conduct several tests for the modified neutral and non-neutral operators separately by using the DNS data [15, 16]. First, in order to examine the effects for the existing seven elliptic operators, let us introduce the general following equation:

$$\alpha_1 f_{ij} - \alpha_2 L\nabla L \circ \nabla f_{ij} - \alpha_3 L^2 \nabla^2 f_{ij} = \frac{\Phi_{ij}^{qh}}{k} + \frac{2b_{ij}}{T} \qquad (19)$$

The set of coefficients of the elliptic relaxation operators is given in Table 1. Each turbulent property of the source term and the length scale are calculated from the DNS data.

The Φ_{ij}^{qh} model, which is very compatible with the elliptic relaxation Eq. [9], is the quasi-linear model of Speziale et al. [17] (hereafter SSG). The SSG model is

$$\begin{aligned}\Phi_{ij}^{qh} &= -(C_1\varepsilon + C_1^* \mathrm{P}_k)b_{ij} + C_2\varepsilon(b_{ik}b_{kj} - \tfrac{1}{3}b_{mn}b_{nm}\delta_{ij}) \\ &\quad + (C_2 - C_3^*\sqrt{B})kS_{ij} \\ &\quad + C_4 k(b_{ik}S_{jk} + b_{jk}S_{ik} - \tfrac{2}{3}b_{mn}S_{mn}\delta_{ij}) \\ &\quad + C_5 k(b_{ik}W_{jk} + b_{jk}W_{ik}) \end{aligned} \qquad (20)$$

$C_1 = 3.4,\ C_1^* = -4.2,\ C_2 = -1.8\ \ C_3 = 0.8 - 1.3\sqrt{B_2},$
$C_4 = 1.25,\quad C_5 = 0.4$

Where the mean rate of the strain and mean vorticity tensors are $S_{ij} = \frac{1}{2}\left(\partial U_i/\partial x_j + \partial U_j/\partial x_i\right)$ and $W_{ij} = \frac{1}{2}\left(\partial U_i/\partial x_j - \partial U_j/\partial x_i\right)$, respectively. The Reynolds stress anisotropy tensor is defined as $b_{ij} = \overline{u_i u_j}/2k - \frac{1}{3}\delta_{ij}$. B_2 $(= b_{ij}b_{jk})$ is its second invariant. The model constants $C_1 \sim C_5$ are used with those of the original model. A symmetry boundary condition of f_{ij} is used at the center of the channel. The wall condition is applied as

$$f_{11} = 0,\ \ f_{22} = -20\nu^2\overline{u_2u_2}/\varepsilon y^4,\ \ f_{33} = 0,$$
and $\ f_{12} = -20\nu^2\overline{u_1u_2}/\varepsilon y^4.$ (21)

In order to confirm the amplification of the redistribution, the present work introduces an amplification tensor factor Γ_{ij} instead of Γ. This factor is defined by

$$\Gamma_{ij} = \frac{kf_{ij}}{\wp_{ij}^{qh}}. \qquad (22)$$

Where the source term $\wp_{ij}^{qh}$ of the elliptic relaxation equation represents the quasi-homogeneous redistribution tensor. This term, which should be modeled, consists of the pressure-strain part and the anisotropy dissipation part. The turbulent properties used in this equation are calculated from the DNS data. The dependent variable f_{ij} is solved from the Poisson equation. Γ_{ij} is able to examine the reduction/amplification effect of the redistribution arising from the elliptic relaxation equation from the wall to the center of the channel. It is one of our primary works to investigate the relationship between the amplification factor and the Reynolds stress. The results will be shown in section 4. Note that it is important for the amplification factor to maintain a neutral value ($\Gamma_{ij} \approx 1$) in the log layer except $\wp_{ij}^{qh} \to 0$ and $kf_{ij} \neq 0$ when using a quasi-homogeneous pressure-strain model which correctly predicts the redistribution in the logarithmic layer. In the near-wall region, it is also necessary for normal components to obtain a value of $\left|\Gamma_{ij}\right| \le 1$ in order to correct the redistribution.

3.2 Length scale in the elliptic operator

Fig. 1 shows the amplification factors Γ_{22} of the wall-normal direction for the redistribution of the original elliptic relaxation equation. The profiles clearly show how the original model is amplified across the channel flow field and how it is affected by the Reynolds number increasing from Re_τ=180 to 590. The trend of the amplification factor is divided into three parts: the near-wall region, the log region and the wake region. First, in the near-wall region (y^+<80; Γ_{22}=1 at y^+=78) the pressure fluctuation is strongly blocked due to the presence of the boundary condition, which will reproduce quite satisfactorily the features of the near-wall flow, as shown by previous works. In the logarithmic region, the amplification factor for Re_τ=590 is increased up to Γ_{22}=1.27 at y^+=167, and then shows a moderate decline in the upper logarithmic layer. However, in the case of Re_τ=180 it is immediately amplified without any gentle decrease of the redistribution because Γ_{22} only has a narrow log region. In the wake

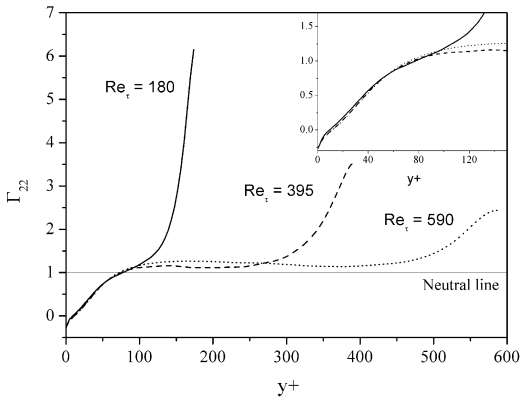

Fig. 1. The profiles of the amplification factor Γ_{22} of the original elliptic relaxation equation using the DNS analysis.

region, it is shown that the amplification factors are again sharply increased from the upper part ($y^+ \approx 400$) of the logarithmic layer up to the center of the channel. In fact, this terrible amplification [fso1] is a decisive motive for this work.

The magnitude of the length scale in the logarithmic layer is decided by its empirical constant C_L and the strength of the kinematic blocking at the wall is related to the constant $C_L C_\eta$ of the Kolmogorov length scale. Here a value of C_η =80, which links a boundary between the turbulent and Kolmogorov length scale, has been used without an objection. Especially, from an analysis of DNS data, Manceau et al. [8] showed that the original value is adequate and reasonable. However, $C_L C_\eta$ has been on occasion changed with the development of each elliptic operator.

In Fig. 2, the effect of this constant is presented by the behavior of the relaxation operator along the wall-normal direction. If $C_L C_\eta$ is much larger than the original value 16, then the redistribution tensor kf_{22} should be underestimated in the near-wall region, as mentioned in Durbin [6]. On the other hand, it can be seen that kf_{22} is strongly amplified in the wake region. The overestimation is probably induced by the over-prediction of wall blocking, which means that the largely predicted eddies by means of the magnitude of the length scale encounter the wall.

The amplification in the wake region is somewhat related to the pressure diffusion D_{22}^p excluded in the source of the elliptic relaxation equation. It is very interesting to examine the effect of D_{22}^p. As previously stated in the original model, the pressure diffusion D_{22}^p is only expressed by its boundary condition, so this term is directly reproduced in the near-wall

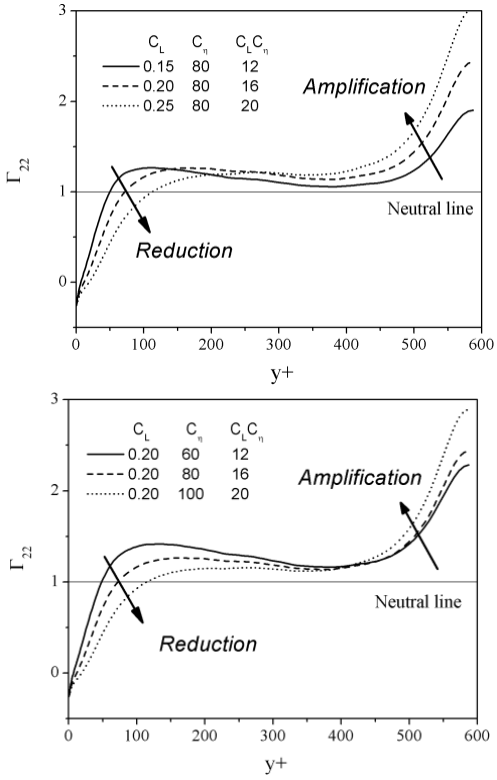

Fig. 2. The effect of the amplification of the redistribution arising from the length scale in the original elliptic relaxation operator.

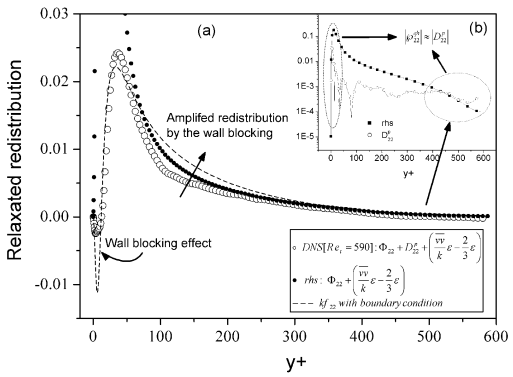

Fig. 3. (a) The wall-blocking effects and the amplification of the redistribution (b) the magnitude comparison between the source term and pressure diffusion, evaluated from the original elliptic relaxation equation using the DNS analyses.

region as shown in Fig. 3(a). In the logarithmic region D_{22}^p is much smaller than $\wp_{22}^{qh}$; thus it is able to be negligible. However, in the wake region the magnitude of D_{22}^p is the same order in comparison with $\wp_{22}^{qh}$ (not Φ_{22}^{qh}) as shown in Fig. 3(b). So D_{22}^p isn't

accurately reproduced by the effect of the boundary condition due to a considerable distance from the wall. Hence, if the exclusion of the pressure diffusion is the reason for the amplification in the wake region, it is not able to be negligible any longer in the source term of the elliptic relaxation equation. Unfortunately, when this term is used in the Reynolds stress transport equation, it is usually absorbed into a gradient transport. Therefore, its own tried-and-true model does not exist explicitly and is only reflected in the value of the empirical coefficient C_μ.

As a result, in the wake region as well as the logarithmic region the amplification of the elliptic operator induces an inaccurate redistribution between the components of the Reynolds stresses. The original elliptic model therefore must be modified by adjusting the elliptic operator or by correcting the source term. Now, note that using a larger length scale at the wall, the constant $C_L C_\eta$ should be carefully adopted.

3.3 Behavior of elliptic operators

As mentioned in part 3.1, the modification of the elliptic relaxation equation is associated with the elliptic relaxation operator (Manceau et al. [8], Wizman et al. [9], Durbin and Laurence [10], Laurence and Durbin [11]) involving the length scale (Pettersson and Andersson [12]). In order to compare these amplification factors of the non-neutral operators (D, M1 and W2) and of the neutral operators (LD, DL, W1 and M2), a standard length scale is used with its original coefficients $C_L = 0.2$ and $C_\eta = 80$. The pressure-strain term in the source term is the SSG model. Also, the original coefficient of both the W1 and M2 models will be examined for 0.29 and 0.28, respectively.

Fig. 4(a) shows the amplification factor Γ_{22} of the elliptic operators given in Table 1. In the logarithmic region, the original model is amplified the largest in comparison with the other operators, as pointed out by Manceau et al. [8, 18]. But the peak value of Γ_{22}^{D} is 1.27, which is lower than 1.51 [8] that is obtained by assuming that the elliptic relaxation equation is not affected by the boundary condition. Two other operators Γ_{22}^{W1} and Γ_{22}^{W2} are predicted with the values of 0.84 and 0.83 at y^+ =220 under the neutral line, respectively. Both models are dependent at the $-2L\nabla^2 L$ term rather than $2(\nabla L)^2$ and $2L^2\nabla L \circ \nabla(1/L)$ in α_1. Fig. 4(b) shows that Γ_{22}^{W2} with $\alpha_1 = 1 - 2L\nabla^2 L \;\; -2L^2\nabla L \circ \nabla(1/L)$, $\alpha_2 = 2$ and $\alpha_3 = 1$ is relatively lower than Γ_{22}^{DL} ($\alpha_1 = 1 - L\nabla^2 L$) and Γ_{22}^{LD} ($\alpha_1 = 1$). The reason is that the W2 operator is strongly affected by $-2L\nabla^2 L$ rather than $-2L^2\nabla L \cdot \nabla(1/L)$ in α_1. Fig. 4(c) shows that, when α_2 increases with $\alpha_1 = 1$ and $\alpha_3 = 1$, Γ_{22}^{LD} ($\alpha_2 = 2$), unlike Γ_{22}^{M1} ($\alpha_2 = 1$) and Γ_{22}^{D} ($\alpha_2 = 0$), is moving towards the neutral line. As regards the effect of the coefficient α_2, it can also be seen that a comparison between the D and M1 models is available. In Fig. 4(d) the W1 (C_L=0.29) and M2 (0.28) models using a larger length scale show that the redistribution is strongly damped in the near-wall and logarithmic layer, and then it is considerably amplified in the wake layer. Now note that the M2 operator is sensitive to the value of β in α_1 and α_2 in the entire region of the channel. If this coefficient is much larger than the neutral constant (β=1/12), Γ_{22}^{M2} will rapidly fall below the neutral line in the $y^+ \approx$ 50~250 region. In this work, β=1/12, which is a standard value for satisfying the neutral operator, is used unless mentioned explicitly.

As a result of the investigation of the elliptic operators through the DNS analyses, the neutral models are comparatively well predicted to the neutral line rather than those of the non-neutral models. However, when the same length scale is used, it can be seen that the prescriptions of the modified elliptic operators are only limited in the logarithmic layer. Therefore, these formulations are not fully free from the amplification of the redistribution in the outer layer in the situation considering a boundary condition. As shown in Fig. 4, the neutral elliptic relaxation operators have been modified significantly, but the results of the DNS

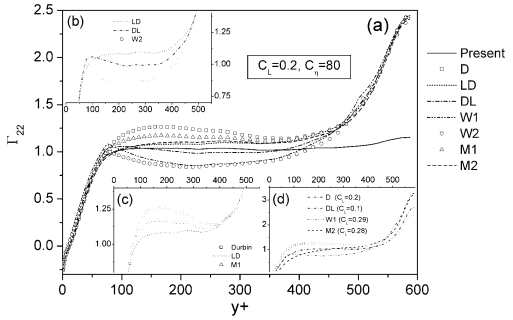

Fig. 4. A comparison of the amplification factors for eight elliptic operators, neutral equations (lines) and non-neutral equations (symbols), using DNS data $Re_t = 590$: (a) The behavior of the amplification factors, (b) The effect of α_1 in logarithmic layer, (c) The effect of α_2 in the logarithmic layer, (d) The effect of the coefficient C_L of original length scale .

analyses indicate that further modifications are required. Unlike the operators proposed so far, the present elliptic operator using the inhomogeneous correction comes close to the neutral line without spoiling the redistribution in the near-wall region as well as the wake region, except for a slight amplification in the core region of the channel. This effect again will be mentioned in part 4.2.

4. Application

For a more thorough check of the agreement of the prior results with the DNS data, we have conducted predictions with the Reynolds stress equation in both the cases of fully developed non-rotating and spanwise rotating channel flows. The Reynolds averaged Navier-Stokes equation and the continuity equation are given by

$$\frac{\partial U_j}{\partial x_j} = 0 , \tag{23}$$

$$\frac{DU_i}{Dt} = -\frac{\partial P}{\partial x_j} + \frac{\partial}{\partial x_j}\left(\mu \frac{\partial U_i}{\partial x_j} - \rho \overline{u_i u_j} \right) - 2\rho \Omega_j U_k e_{ijk} . \tag{24}$$

The governing equations are closed with the Reynolds stress transport equation $\overline{u_i u_j}$.

$$\frac{D\overline{u_i u_j}}{Dt} = (P_{ij} + R_{ij}) + (D_{ij}^{v} + D_{ij}^{t} + D_{ij}^{p}) + \wp_{ij} - \frac{\overline{u_i u_j}}{k}\varepsilon \tag{25}$$

where

$$P_{ij} = -\left(\overline{u_k u_i} \frac{\partial U_j}{\partial x_k} + \overline{u_k u_j} \frac{\partial U_i}{\partial x_k} \right), \tag{26}$$

$$R_{ij} = -2\Omega_k \left(\overline{u_j u_m} \quad e_{ikm} + \overline{u_i u_m} \quad e_{jkm} \right), \tag{27}$$

$$D_{ij}^{v} = \frac{\partial}{\partial x_k}\left(\nu \frac{\partial \overline{u_i u_j}}{\partial x_k} \right), \tag{28}$$

$$D_{ij}^{t} + D_{ij}^{p} = \frac{\partial}{\partial x_k}\left(\frac{C_\mu}{\sigma_k} \overline{u_k u_m} \quad T \frac{\partial \overline{u_i u_j}}{\partial x_m} \right). \tag{29}$$

P_{ij} , R_{ij} are the generations by the mean shear and by the system rotation, respectively. The effects of rotation are produced through a rotational production term which appears not only in the momentum equation governing the mean flow but also in the transport equations governing the Reynolds-stress tensor. D_{ij}^{v} , D_{ij}^{t} and D_{ij}^{p} are the laminar viscous, turbulent and pressure diffusion, respectively. $\wp_{ij}$, which was mentioned in section 2, is the redistribution tensor and the final term $\overline{u_i u_j}\varepsilon/k$ is the anisotropy dissipation rate tensor.

The model equation for the Reynolds stresses are finally closed with the transport equation for the dissipation rate ε of the turbulent kinetic energy,

$$\frac{D\varepsilon}{Dt} = \frac{C_{\varepsilon 1} P_k - C_{\varepsilon 2}\varepsilon}{T} + \nu \frac{\partial^2 \varepsilon}{\partial x_j \partial x_j} + \frac{\partial}{\partial x_i}\left(\frac{C_\mu}{\sigma_\varepsilon} \overline{u_i u_j} T \frac{\partial \varepsilon}{\partial x_j} \right), \tag{30}$$

For the closure of ε and $\overline{u_i u_j}$, the constants used here are

$$C_\mu = 0.26, \quad C_{\varepsilon 1} = 1.35(1 + 0.1 P_k / \varepsilon), \quad C_{\varepsilon 2} = 1.83,$$
$$\sigma_k = 1.0, \quad \sigma_\varepsilon = 1.3.$$

The numerical scheme uses the well-established finite-volume method. The dependent variables are solved by TDMA. No-slip boundary conditions at the solid walls are $U_i = 0$, $\overline{u_i u_j} = 0$ and $\varepsilon = 2\nu k / y^2$. The elliptic relaxation equation is given in Section 3. For the source term of the elliptic relaxation equation the quasi-homogeneous pressure-strain correlation is the SSG model. The results are normalized with the friction velocity. The value of y^+ at the node nearest to the walls is located at about 0.25 based on a non-rotating flow for all of the test cases. The grid expansion is applied towards the center of the channel and its rate is about 1.02.

4.1 Non rotating channel flow

In the plane channel flow Re_τ =180, Fig. 5 shows the amplification factor for all four different elliptic relaxation models (Present, D, W1 and M2). In order to test the effect of the length scale, the W1 and M2 operators, which are originally modeled with C_L = 0.28, and 0.29, respectively, are additionally calculated for $C_L = 0.2$ with $C_\eta = 80$. The reason for the additional test is that C_L in the elliptic operator was very sensitive from the DNS analyses of the previous section. Before referring to the mean velocity and turbulent properties, it is important to examine the amplification factor of the wall-normal component that directly has an effect on the wall blocking away from the wall. It is shown that the trend of the amplification factors is almost similar to the results of the previous sections by using the DNS data. That is, Γ_{22}^{D} is the most amplified, whereas Γ_{22}^{W2} is predicted as the lowest. In Fig. 5(b) all four profiles of Γ_{11} , which receives turbulent energy from the reduction of the wall-normal redistribution due to a wall-blocking

effect, is very similar to those of Γ_{22}.

The amplification factors for the shear component are also illustrated in Fig. 5(c). It can be seen that the present and D models reproduce the neutral line without an amplification of the redistribution in the outer layer very well. Whereas Γ_{12}^{W1} is gently damped. This feature is also apparent in Γ_{12}^{M2}, which reacts weakly in comparison with the amplification of the normal components.

As regards the effect of the length scale, an evident result is that, by increasing the $C_L C_\eta$ constant, the amplification of the redistribution is induced in the whole region, unlike the behavior of the elliptic operator that is only dependent around the logarithmic region.

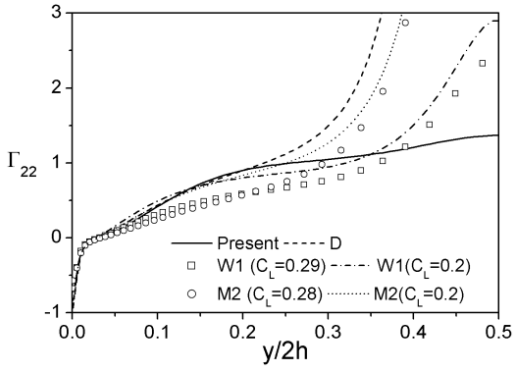

(a)

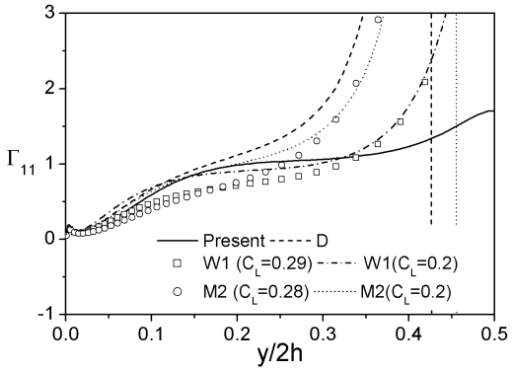

(b)

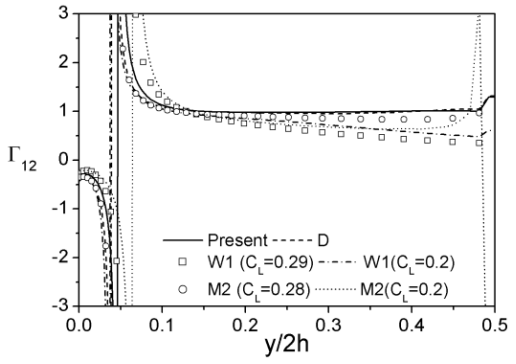

(c)

Fig. 5. Comparison of the amplification factors of the redistribution by the four elliptic operators at Re_t=180 in the channel flow.

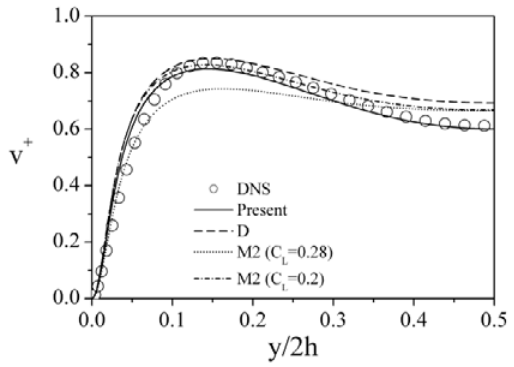

(a)

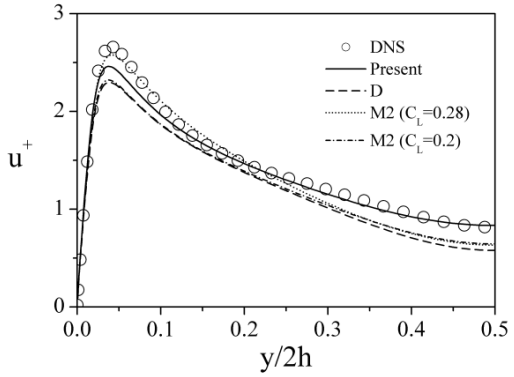

(b)

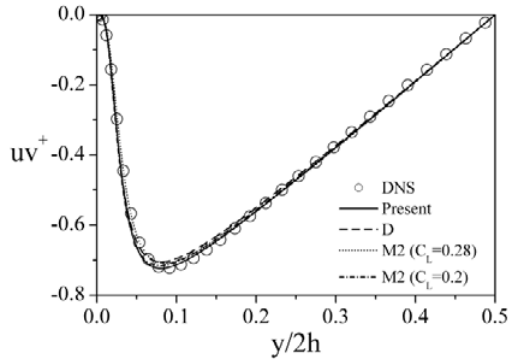

(c)

Fig. 6. Comparison of Reynolds stress components calculated from three operators with the DNS data Re_t=180 in the channel flow.

In Fig. 6 the profiles of the Reynolds stress components for all four tests of the three operators (Present, D, M2) are compared with the DNS data [8] $Re_t = 180$. In the inner layer Fig. 6(a) shows that the wall-normal component v^+ for all of the models agrees very well with the DNS except for M2 with C_L =0.28. It can be seen that although the M2 model using the coefficient C_L =0.28 is substantially underpredicted, the result using 0.20 gives a reasonable prediction. The profile v^+ of the D model is overpredicted in comparison with the DNS data in the overall region. This result is directly related to the underprediction of the streamwise component as shown in Fig. 6(b). Both normal stresses of the M2 model (C_L =0.2), which have a smaller amplification of the redistribution than those of D model, are slightly improved due to the α_1 and α_2 coefficients of the elliptic relaxation equation. The present model keeps better track of the DNS than the other operators in the whole region. Fig. 6(c) shows that the results of the four operators for the shear component uv^+ agree very well with the DNS data.

As a result, it can be seen that the neutral parameter $(1-\sigma) = 4B_2$ correctly eliminates the amplification of the redistribution arising from the elliptic operator in the outer layer. The energy transfer of the wall-normal redistribution component has an effect on two other normal Reynolds stresses since the sum of the normal redistribution components becomes zero in the main region of the flow. Therefore, it can be concluded that present model is able to obtain improved results by almost perfectly eliminating the amplification. This can again be explained by the result that the correct prediction of the present model for the mean velocity is improved more than the original model in both the logarithmic and wake regions, as shown in Fig. 7.

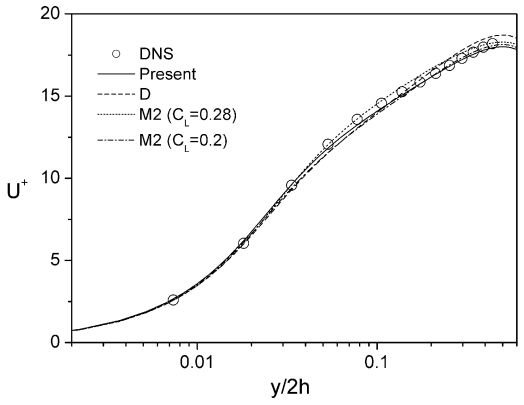

Fig. 7. Comparison of the streamwise velocity calculated from four operators with the DNS data Re_t =180 in the channel flow.

4.2 Rotating channel flow

In the simulations for the rotating channel flows using the elliptic relaxation method, Wizman et al. [9] and Pettersson & Andersson [12] by using their modified elliptic models were successfully able to apply them with an additional source term in the dissipation rate transport equation. According to Wizman et al. [9], in the near-wall region the agreement with the DNS was only satisfactory when the additional term was explicitly introduced into the dissipation equation, not from the elliptic relaxation equation. On an examination for the dissipation rate of an isotropic turbulence, moreover, Speziale [19] demonstrated that the additional term in the dissipation rate equation is not only theoretically unfounded but it is also limited at a local rotation number. Hence, the use of an additional term can induce unphysical phenomena on industrial applications since it is purely empirical. In the present calculations, where no additional terms in the governing equation as well as the dissipation rate equation are used, the rotation effects are induced only from the rotational production and the absolute vorticity of the pressure-strain term in the Reynolds stress equation.

In order to evaluate the performance of the present elliptic operator for the spanwise rotating channel flows, the computational results are compared with the three DNS/LES data: Kristoffersen & Andersson [13] (hereafter, KA-DNS) for Re_t=194 and $Ro(=2h\Omega/U_B)$ = 0.0 to 0.5; Piomeli & Liu [14] (PL-LES) at $Re_t = 320$ =320 and $Ro = 0.21$ =0.21; and also El-Samni & Kasagi [20] (EK-DNS) at $Re_t = 150$ =150 and $Ro = 1.0$ =1.0.

Fig. 8(a) shows that the wall-normal redistributions $\wp_{22}$ $(= kf_{22})$ of the present operator along with three different ones (D, LD and W2) are compared with the KA-DNS data for $Re_t = 197$ and Ro =0.15. The D model shows that the profile of kf_{22} is overestimated on the suction side, which exhibits a relaminarization, and is underestimated at the pressure side. The LD operator, which predicted a lower amplification in the logarithmic layer, gives a better prediction at the suction side in a comparison with that of the original model. But the redistribution of this operator is still

overestimated. To be noted is the fact that, in the main part of the channel, the result of the DNS data has a large negative distribution, whereas those of the three elliptic models are positive. This same result was also observed at higher rotation numbers. It is interesting that the gap between the present prediction and the DNS data balances the pressure diffusion D_{22}^{p} and it has almost a similar magnitude in comparison with the redistribution term in Fig. 8(a). Although the pressure diffusion in the outer layer is absorbed into the gradient transport through the model coefficient C_{μ}, its effect is also presented by the boundary condition of the elliptic relaxation equation. In particular, in Fig. 8(b) it can be seen that their amplification factors are violently fluctuating in the range of $y/2h \approx$ 0.3~0.8. Subsequently, the wall-normal components of the redistribution are not correctly predicted in the whole region. The results for these operators are induced by the spurious behavior of the elliptic operators in the outer layer.

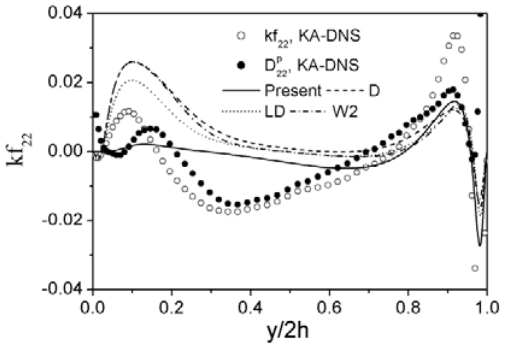

(a)

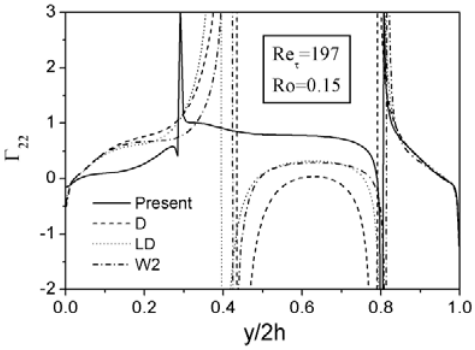

(b)

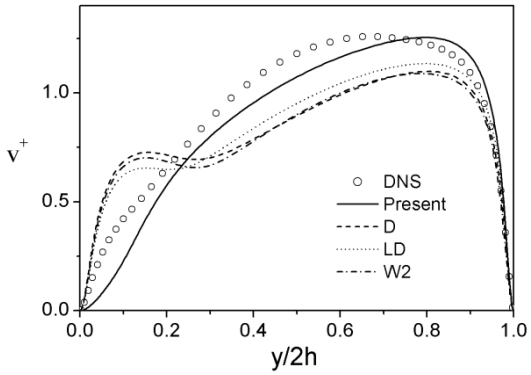

(c)

Fig. 8. The comparison of four operators in a rotating channel flow at $Re_t = 197$ and $Ro = 0.15$: (a) The wall-normal redistribution tensor kf_{22}, (b) the amplification factor of redistribution tensor, (c) wall-normal stress.

In Fig. 8(b) it can be seen that the present model keeps to the neutral line in the rotating flow. Whereas, the amplification factor Γ_{22} of the D, LD and W2 models is highly sensitive in the main region of the channel. Therefore, unless these problems are solved in the rotating flow these results of the elliptic relaxation models will fail to obtain good predictions. In Fig. 8(c) the profiles of the normal Reynolds stress component are shown. The present model slightly underestimates them in comparison with KA-DNS on the suction side, whereas it gives an improved prediction at the other side. As shown in the previous section, we see that the elimination of the amplification leads to a satisfactory result without using any additional term in order to obtain a rotation effect.

In Fig. 9, the redistribution tensor $\wp_{ij}(=kf_{ij})$ of the Reynolds stresses obtained by the present elliptic relaxation operator is compared with the KA-DNS data for two rotation numbers, $Ro = 0.15$ and 0.5. The profile of the streamwise component kf_{11} in Fig. 9(a) is fairly well reproduced for both rotation numbers on the pressure side, except for an underprediction on the suction side. This trend also is shown in the other two normal components in Fig. 9(b) and (c). In Fig. 9(d), it is clear that the profile of kf_{12} is quite well represented in the overall region in comparison with the DNS data. It can be seen from these results that the present elliptic operator is able to predict the correct trend. This model is capable of exhibiting a relaminarization in the suction side without an overestimation of the redistribution, which causes a fallacious amplification of the elliptic operator in the region of a lower Reynolds number.

Fig. 10(a) shows the mean velocity predictions normalized by the bulk velocity by using three different rotation numbers $Ro = 0.0$, 0.15 and 0.5. The peak point of the mean velocity is shifted towards the suction side of the channel with an increase of the

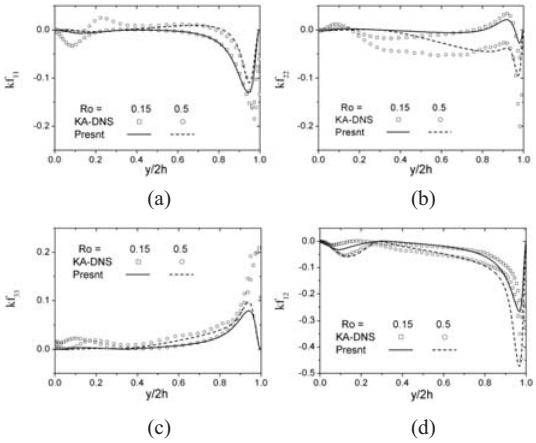

Fig. 9. The relaxed redistribution tensor compared with the KA-DNS data $Re_t = 197$, $Ro = 0.15$ and 0.5 in rotating channel flow.

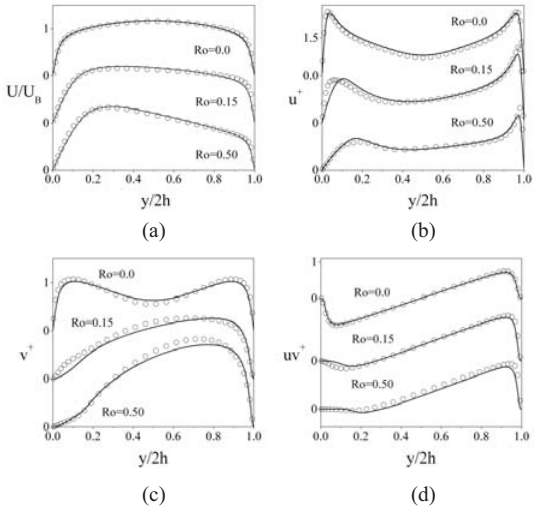

Fig. 10. The results computed from the three different rotation numbers at $Re_t = 197$ in the rotating channel flow: (a) Mean velocity, (b) streamwise stress component, (c) well-normal stress component, (d) shear stress component.

otation number. The profiles show that the width of the linear slope region increases with the rotation number, and the predictions of the present model compare well with the DNS data. Figs. 10(b)-(d) present the profiles of the Reynolds stress normalized by a friction velocity. The streamwise stress component u^+ corresponds to the DNS data in the suction side. When the rotation rates are increased, the wall-normal stress v^+ is gradually increased in the overall region, and is correctly predicted at the suction side, as shown in Fig. 10(c). In Fig. 10(d) the positions of zero shear stress are shifted from the center of the channel towards the suction side when the rotation numbers are increased. Overall, the present model for an imposed system rotation shows good agreement with the DNS data at higher rotation numbers. The capture of a relaminarization by the present computation is a significant result since the present elliptic relaxation model is obtained without using any additional empirical source term in the governing equations as well as the dissipation rate equation.

Figs. 11(a)-(c) are to present the normal Reynolds stresses compared with the three DNS/LES results, that is, the PL-LES, KA-DNS and EK-DNS. For a higher Reynolds number $Re_t = 320$ and $Ro = 0.21$, the three normal components show a good overall agreement with the PL-LES data except for a slight discrepancy in the core region of the channel. In comparison with KA-DNS, three normal stresses of this model are quite well predicted, but the spanwise component is slightly underpredicted in the overall region. For a lower $Re_t = 150$ and a higher $Ro = 1.0$, we have performed another computation with EK-DNS data. As shown in Fig. 11, although some differences exist in the magnitude of the three normal Reynolds stresses in comparison with EK-DNS, it can be seen that the present model, which is not using an ad hoc additional rotating source, can be applied to higher rotation numbers without serious numerical instability.

For numerical stability, when the computation of the original elliptic relaxation equation with the RSM is performed in the application with a complex flow, some users adopting this model have often suffered from a numerical instability from its boundary condition. Especially, in a fully developed two-dimensional channel flow, the shear component f_{12} is numerically unstable since in the near-wall region the boundary condition of f_{12} behaves as $1/y$. In this work this numerically unstable issue has appeared in computing the flow of lower Reynolds numbers and higher rotation numbers such as the EK-DNS test. The reason for this seems to be associated with the small amplification of the redistribution in the wake region: By increasing the rotation number, due to the stronger relaminarization on the suction side, the amplification/reduction of the redistribution fluctuates more violently than that of the pressure side. At this time, the behavior of the spurious redistribution is physically violated from natural law. As a result, the f_{12} equation diverges. Here this issue is carefully solved by adjusting the time step and its iteration

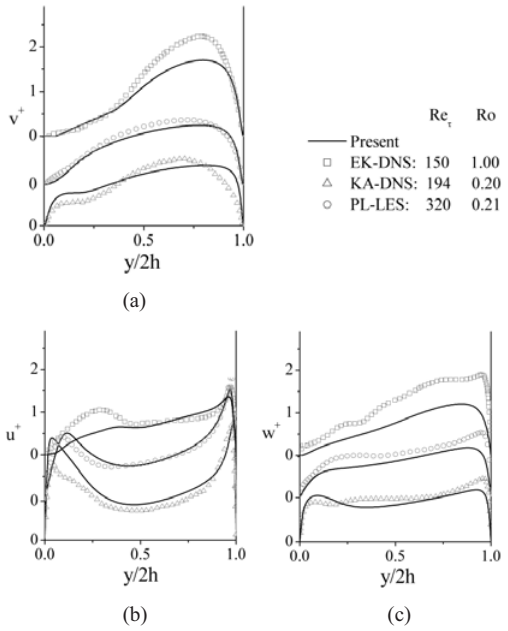

Fig. 11. Normal Reynolds stresses compared with DNS/LES data for the three different Reynolds numbers and rotation numbers.

number.

5. Conclusions

Reynolds stress transport modeling in conjunction with the elliptic relaxation approach as a near-wall RANS model is the method to correct the redistribution term down to solid walls. It has led to very encouraging results for simple flow fluids such as the fully developed plane channel flow. The important key of these results is the wall blocking effect that suppresses the velocity fluctuations primarily in the wall-normal direction and creates the inhomogeneous and anisotropic turbulence in the near-wall layer and the lower part of logarithmic region. However, from the present work it can be clearly seen that the amplification effect of the redistribution, which is induced by the wall blocking, extends into the core region of the channel, and then the behavior of the redistribution is violently amplified in the outer layer including the wake region.

The amplification effects of the elliptic relaxation equation are investigated for the elliptic operators and their length scale. The behavior of the amplification factor from the elliptic operators shows that the redistribution of the non-neutral operators such as Durbin's original model is amplified more than that of the neutral operators in the logarithmic layer. However, the modifications of these neutral operators are only induced in the logarithmic region. All of the elliptic operators are dependent on the Kolmogorov length scale in the near-wall region. The behavior of the redistribution for its constant $C_L C_\eta$ is very sensitive. In particular, the effects in rotating flows are more sensitive when increasing the relaminarization on the suction side of the channel. It is related to the numerical instability from an unphysical phenomenon of the redistribution.

The present elliptic operator removes almost all the amplification of the redistribution in the outer layer. At the channel flow, this model is applied with good results. Moreover, the present formulation shows good agreement with the DNS data for a wide range of rotation numbers without adopting an additional empirical source term in the dissipation rate equation.

Aknowlegements

This work was supported by Korea Science and Engineering Foundation (grant No. R05-2003-000-12391-0) grant No. R01-2003-000-10571-0). We are grateful for the specific comments and suggestions from the reviews.

Nomenclature

b_{ij}	:	Reynolds stress anisotropy
B_2	:	Second invariant
C	:	Turbulence model constant
C_L	:	Length scale constant
C_T	:	Time scale constant
C_η	:	Time scale constant
D_{ij}	:	Diffusion of $\overline{u_i u_j}$
e_{ijk}	:	Permutation tensor
f_{ij}	:	Intermediate variable
h	:	Channel half width
k	:	Turbulent kinetic energy
P	:	Mean static pressure
p	:	Pressure fluctuation
P_{ij}	:	Production rate of $\overline{u_i u_j}$
P_k	:	Production rate of k
Re_t	:	Reynolds number
Ro	:	Rotation number
S_{ij}	:	Mean rate of strain tensor
T	:	Turbulent time scale
R_{ij}	:	Production rate of $\overline{u_i u_j}$ by system rotation
U_i	:	Mean velocity
u_i	:	Fluctuating velocity

$\overline{u_i u_j}$: Reynolds stress
y^+ : Wall normal distance
W_{ij} : Mean vorticity tensor

Greeks

α : Constant of elliptic relaxation equation
δ_{ij} : Kronecker delta
ε : Dissipation rate of k
ε_{ij} : Dissipation rate tensor
ν : Kinematic viscosity
ρ : Density
σ : Intermediate parameter
σ_k : Model constants of $\overline{u_i u_j}$
σ_ε : Model constants of ε
Ψ_{ij} : Two point correlation
Φ_{ij} : Pressure strain or redistribution
Γ : Amplification factor of f_{ij}
Γ_{ij} : Amplification tensor factor of kf_{ij}
Π_{ij} : Velocity-pressure gradient correlation
Ω : Angular rotation rate
$\wp_{ij}$: Relaxed redistribution

Superscript

$+$: Normalization parameter
h : Homogeneous
inh : Inhomogeneous
p : Pressure part
qh : Quasi homogeneous
t : Turbulent part

References

[1] P. Y. Chou, On velocity correlations and the solutions of the equations of turbulent fluctuation, Q. Appl. Maths **3** (1945) 38.

[2] J. C. Rotta, Statistische Theorie nichthomogene Turbulenz, Z. Phys. 129 (1951) **547**.

[3] B. E. Launder and D. P. Tselepidakis, Contribution to the modeling of near-wall turbulence, Turbulent Shear Flows Vol. **8**, Springer, Berlin, (1993).

[4] B. E. Launder and S.-P. Li, On the elimination of wall-topography parameters from second-moment closure, *Phys. Fluids* **6** (1994) 999.

[5] T. J. Craft and B. E. Launder, A Reynolds stress closure designed for complex geometries, *Int. J. Heat Fluid Flow* 17 (1996) 245.

[6] P. A. Durbin, Near-wall turbulence closure modeling without damping function, Theoret. Comput. *Fluid Dynamics*. **3** (1991) 1.

[7] P. A. Durbin, A Reynolds stress model for near-wall turbulence, *J. Fluid Mech*. **249** (1993) 465.

[8] R. Manceau, M. Wang and D. Laurence, Inho mogeneity and anisotropy effects on the redistribtion term in RANS modeling, *J. Fluid Mech*. **437** (2001) 307.

[9] V. Wizman, D. Laurence, M.Kanniche, P. Durbin and A. Demuren, Modeling near-wall effects in second-moment closures by elliptic relaxation, *Int. J. Heat and Fluid Flow* **17** (1996) 255.

[10] P. A. Durbin and D. Laurence, Nonlocal defects in single point closure. Proc. Third Turbulence Research Association Conf. Seoul, Korea, (1996).

[11] D. Laurence and P. Durbin, Modeling near wall effects in second moment closure by elliptic relaxation, Proceedings of the Summer Program, CTR, Stanford University/NASA Ames Research Center, (1994).

[12] B. A. Pettersson and H. I. Andersson, Near-wall Reynolds-stress modeling in noninertial frames of reference, Fluid Dynamics Research **19** (1997) 251.

[13] R. Kristoffersen and H. I. Andersson, Direct simulations of low Reynolds number turbulent flow in a rotating channel, *J. Fluid Mech*. **256** (1993) 163.

[14] U. Piomelli and J. Liu, Large-eddy simulation of rotating channel flow using a localized dynamic model, *Phys. Fluids* **7** (1995) 839.

[15] J. Kim, P. Moin and R. D. Moser, Turbulence statistics in fully developed channel flow at low Reynolds number*, J. Fluid Mech*. **177** (1987) 133.

[16] R. D. Moser, J. Kim and N. N. Mansour, Direct numerical simulation of turbulent channel flow up to $Re_t = 590$, *Phys. Fluids* **11** (1999) 943.

[17] C. G. Speziale, Turbulence modeling in noninertial frames of reference, *Theoret. Comput. Fluid Dyn*. **1** (1989) 3.

[18] R. Manceau and K. Hanjalic, A new form of the elliptic relaxation equation to account for wall effects in RANS modeling, *Phys. Fluids* **12** (2000) 2345.

[19] C. G. Speziale, S. Sarkar and T. B. Gatski, Modeling the pressure-strain correlation of turbulence: an invariant dynamical systems approach*, J. Fluid Mech*. **227** (1991) 245.

[20] O. A. El-Samni and N. Kasagi, The effects of system rotation with three orthogonal rotating axes on the turbulent channel flow. Proc. 7th Int. Conf. On Fluid Dynamics and Propulsion, 19-21 December, Sharm El-Sheik, Egypt, (2001) 1-7.